Biointerface Research in Applied Chemistry
Open-Access Journal (ISSN: 2069-5837)

Article
Volume 14, Issue 6, 2024, 129
https://doi.org/10.33263/BRIAC146.129

Molecular Docking and Hepatoprotective Evaluation of Jackfruit Leaf (*Artocarpus heterophyllus* Lam.) in Rat Induced Isoniazid and Rifampin

Ira Asmaliani [1,*], Sukmawati [1], Andi Trihadi Kusuma [2], Muammar Fawwaz [2,*]

[1] Laboratory of Pharmacology, Faculty of Pharmacy, Universitas Muslim Indonesia, Makassar 90231, Indonesia
[2] Laboratory of Pharmaceutical Chemistry, Faculty of Pharmacy, Universitas Muslim Indonesia, Makassar, Indonesia
* Correspondence: muammar.fawwaz@umi.ac.id;

Scopus Author ID 56085116100
Received: 27.06.2024; Accepted: 6.10.2024; Published: 10.12.2024

Abstract: Isoniazid and rifampin are antituberculosis drugs with a side effect in hepatotoxicity. An antioxidant can neutralize the toxic effects of these drugs on the liver. Jackfruit leaf (*Arthocarpus heterophyllus* Lam.) was identified as a rich source of antioxidants. This study aims to determine the effect of the ethanolic extract of jackfruit leaf (EEJL) on the liver histopathological structure of the rats induced by isoniazid-rifampin and analyze the molecular docking interaction of *Arthocarpus heterophyllus* Lam. active compound toward targeted receptor. The histological structure was determined using the Hematoxylin-Eosin staining method. Fifteen male Wistar rats were divided into five groups. Group 1 is a negative group with 1% sodium carboxymethyl cellulose. Group 2, as a positive control, was given a Curliv®, and the treatment groups 3, 4, and 5 were given EEJL at a dose of 100, 200, and 300 mg/kg body weight (BW), respectively. Before being treated, the rats were induced with an isoniazid-rifampin dose of 300 mg/kg BW orally for three days. The extract was administered orally once a day for seven days. On the eighth day, the liver was collected for histologic observation. Molecular docking was performed using the AutoDock Vina package to estimate the interaction of the ligand-receptor complex using 1HD2 and 3NT1 corresponding to antioxidant and COX-1 receptors, respectively. The results revealed that the treatment of EEJL affected repairing the structure of damaged liver cells in rats. Histological observation revealed that the group dose of 300 mg/kg BW had a better effect than other groups because only sinusoid dilatation was seen in the liver section. The molecular docking study showed that the ΔG produced between the test ligands toward 1HD2 is at a lower level (-6.134 to -6.881 kcal/mol) compared to the native ligand, which is only -4.701 kcal/mol. Besides, the interaction of test ligands toward targeted receptor 3NT1 exhibited a higher level than the native ligand. Therefore, the EEJL has shown significant improvement in the histology of rat liver, which might be due to its high stability interaction of active compounds toward 1HD2 and 3NT1 corresponding to antioxidant and COX-1 receptors, respectively.

Keywords: docking; isoniazid; jackfruit; rifampin; histopathology.

1. Introduction

Tuberculosis (TB) is caused by Mycobacterium tuberculosis and is commonly found in developing countries, particularly in Southeast Asia, including Indonesia. Long-term TB treatment may cause drug-induced liver injury (DILI). DILI is a condition where liver damage is caused by the consumption of drugs, dietary supplements, and their metabolites. The

incidence rate of DILI has been increasing every year [1,2], and it is currently the fifth leading cause of death due to liver diseases worldwide [3]. Therefore, DILI has garnered significant attention in the medical field.

Isoniazid and rifampin are the primary drugs used in treating tuberculosis. However, their use can lead to liver injury, which can cause liver failure, accounting for 5%–22% of acute liver failure cases [4]. The precise cause of isoniazid-induced liver injury is not yet fully understood. However, the mechanisms behind this liver injury mainly involve several factors, such as oxidative stress, mitochondrial dysfunction, drug metabolic enzymes, protoporphyrin IX accumulation, endoplasmic reticulum stress, bile transport imbalance, and immune response. One theory suggests that isoniazid leads to oxidative stress injury due to the dysregulated compensatory activation of the nuclear erythroid 2-related factor 2/antioxidant response element (Nrf2/ARE) antioxidant stress system and the accumulation of reactive oxygen species (ROS) [5]. Rifampin is also known to be associated with endoplasmic reticulum stress and the accumulation of lipids in the liver [6]. Cholestasis is the primary cause of liver injury due to rifampin, characterized by increased bile acid synthesis and decreased bile acid transport [7].

Natural medicinal ingredients have unique advantages in improving patients' symptoms, reducing the risk of liver injury, delaying the progress of liver injury, and enhancing the body's repair ability. They have the characteristics of multi-level, multi-target, and multi-channel comprehensive regulation. In recent years, natural medicinal ingredients have been shown to have a good protective effect on liver injury caused by isoniazid and rifampicin [8]. Antioxidants of natural medicine can neutralize the toxic effects of drugs on various organs. Several studies have shown that various antioxidants in medicinal plant extracts can suppress oxidative stress in experimental animals [9]. Medicinal plant extracts mainly act as free radical scavengers, forming complexes with metals (metal chelation) and stabilizing membrane systems [10,11].

One of the plants identified as a rich source of antioxidants is jackfruit leaves (*Arthocarpus heterophyllus* Lam). Jackfruit leaves contain tannins, flavonoids, steroids, saponins, and glycosides [12]. Ethanolic extract of jackfruit leaves (EEJL) has antioxidant activity in the DPPH method with an IC_{50} value of 48.09 µg/mL [13]. These results indicated that the EEJL has powerful antioxidant activity. Therefore, we aim to determine the effect of the jackfruit leaf extract on the liver histopathological structure of the rats induced by isoniazid and rifampin. Furthermore, we will conduct molecular docking analysis of several steroid compounds in *Arthocarpus heterophyllus* Lam.

The effect of EEJL on the liver histopathological structure was determined in the divided animal group using positive and negative controls. Molecular docking was performed using the AutoDock Vina package to estimate the ligand's interaction with the antioxidant and COX-1 receptor complex. This preliminary study is for developing an herbal medicine for companion TB patient therapy, particularly for protecting the liver from potential damage caused by prolonged use of TB drugs.

2. Materials and Methods

2.1. General.

The solvents and other chemicals were of analytical grade. Deionized water was obtained through a Millipore-Q50 Ultrapure water system (Sartorius, USA). Ethanol 96%,

sodium carboxymethyl cellulose (Na CMC), xylene, paraffin, formalin buffer, hematoxylin-eosin dye, and entellan were purchased from Sigma Chemicals Co. (St. Louis, MO, USA). Curliv® tablet (Soho Industry, Indonesia) is the natural hepatoprotector from curcumin, which was used as a positive control. Isoniazid and rifampin were purchased commercially (Kimia Farma, Indonesia).

2.2. Sample preparation.

The jackfruit leaves were collected from Makassar, South Sulawesi, Indonesia. The leaf was identified in the Laboratory of Natural Products, Faculty of Pharmacy, Universitas Muslim Indonesia, Makassar, Indonesia. Jackfruit leaves were sorted, dried, and powdered. The sample powder was extracted by maceration at room temperature using ethanol for 3 × 24 h. Subsequently filtered, re-maceration was carried out until the extraction was complete. The filtrate was collected and concentrated through a vacuum evaporator to obtain a thick ethanol extract, and then fresh drying was used to obtain a dry extract.

2.3. Animal model.

This study used adult male Wistar rats (weighing between 150 and 200 g). They were fed a typical commercial pellet diet and given access to unlimited water. The rats were first adapted for one week before being divided into five groups. Group 1 received 1% Na.CMC suspension; Group 2 received Curliv® suspension at a dose of 15.595 mg/kg BW; and Groups 3, 4, and 5 received EEJL doses of 100 mg/kg BW, 200 mg/kg BW, and 300 mg/kg BW, respectively. All test animals were given 300 mg/kg BW of isoniazid-rifampin orally over three days. Following that, the extract was given orally once each day for seven days. The animals were then sacrificed on the eighth day, and their livers were separated. The liver was then prepared for microscopic analysis using histology approaches, which included congestion, hydrophilic degeneration, fatty degeneration, sinusoidal dilatation, damaged blood vessels, and necrosis. Animal studies at Universitas Muslim Indonesia followed the laboratory's animal care and use protocols.

2.4. Histopathology.

The liver from each rat was removed and fixed in 10% formalin buffer. The specimens were processed for dehydration using ethanol, clearing in xylene, and impregnation with molten paraffin wax in an oven at 60°C using an automatic tissue processor. Next, the tissues were embedded using an embedding station (4-5 µm), cut, and stained with hematoxylin-Eosin. The specimens were examined using optical microscopes. An experienced pathologist performed all subsequent histopathological examinations [14,15].

2.5. Molecular docking.

In this study, we used the AutoDock Vina package for molecular docking to predict the interaction of the ligand-receptor complex [16]. Molecules were obtained from the PubChem database. The ligand was downloaded and saved in SDF format. The chemical structures of ligands are shown in Figure 1, which are steroid compounds contained in *Arthocarpus heterophyllus* Lam [17]. In receptor preparation, the three-dimensional structure was obtained from the RCSB database with PDB ID 1HD2 and 3NT1 corresponding to antioxidant and COX-1 receptors, respectively. The receptor was saved in PDBQT format after computing the

polar hydrogen and Kollman's united atom charges to the receptor. All docking results were then processed and visualized in Open-Source PyMOL v 2.3 software [18].

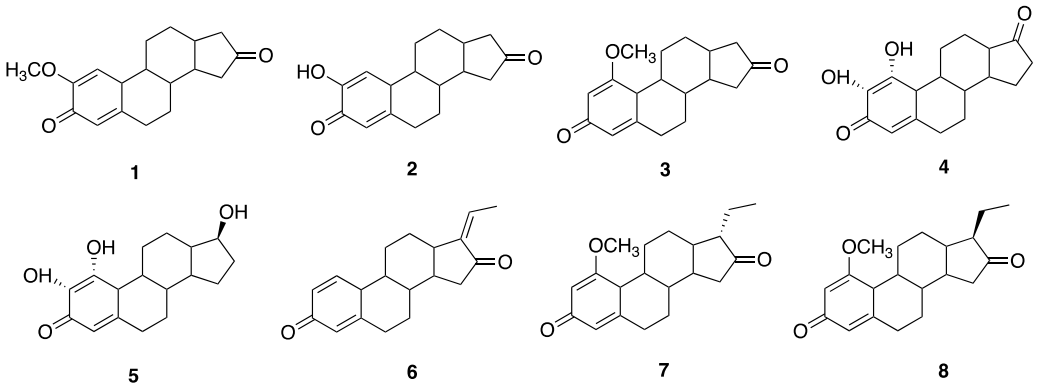

Figure 1. Chemical structure of steroid compounds contained in *Arthocarpus heterophyllus* Lam.

3. Results and Discussion

3.1. Histopathology.

The effect of EEJL on the histological appearance of the liver in rats (Rattus norvegicus) treated with isoniazid-rifampin. Histological analysis was performed under a microscope to see how isoniazid and rifampin improved the structure of liver cells following EEJL treatment. Figure 2 shows the results of the histological study.

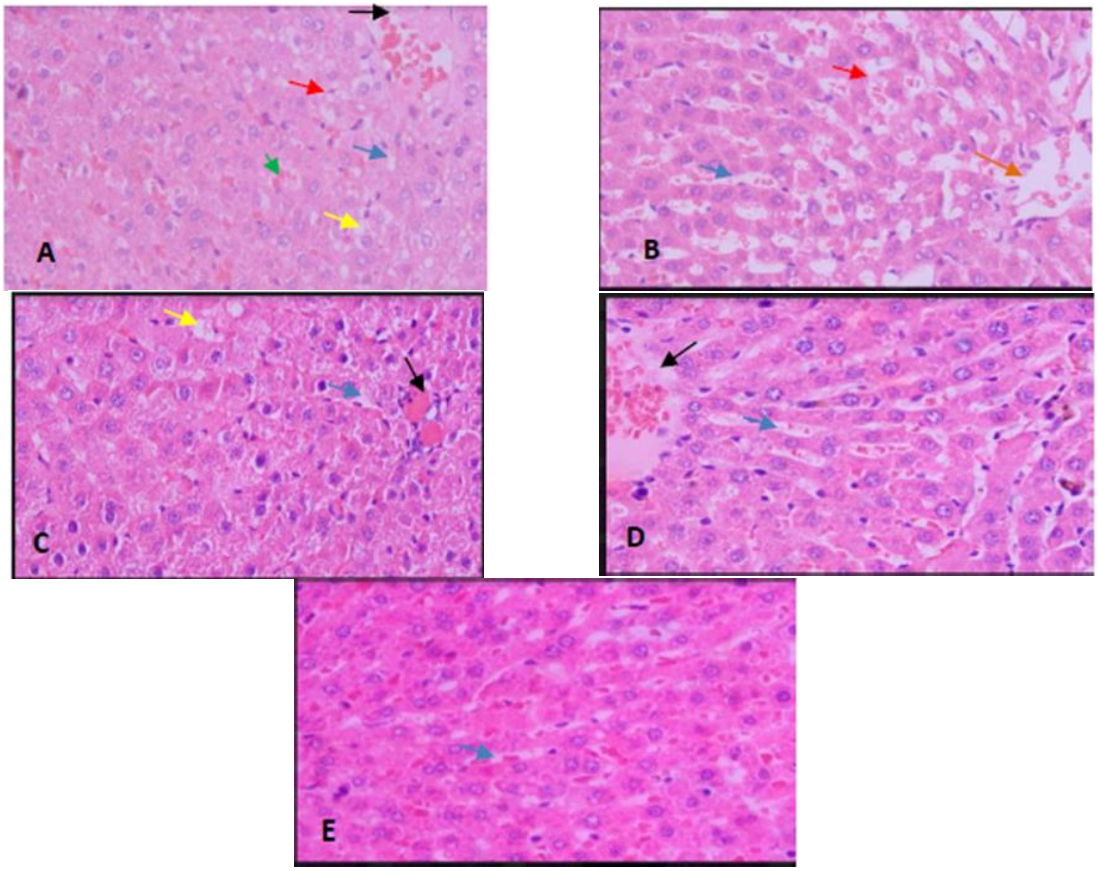

Figure 2. Histopathological description of rat liver. **(A)** Negative group (Na.CMC 1%); **(B)** Positive group (Curliv®); **(C)** EEJL 100 mg/kg BW; **(D)** EEJL 200 mg/kg BW; **(E)** EEJL 300 mg/kg BW. Dilated sinusoids (blue arrow); hydrophilic degeneration (yellow arrow); fat degeneration (red arrow); sinusoidal congestion (green arrow); congestion (black arrow); inflammation (orange arrow).

Jackfruit leaves contain alkaloids, tannins, flavonoids, steroids, saponins, carbohydrates, and glycosides [17,19]. Jackfruit leaves can be used as a natural antioxidant because of their secondary metabolites. EEJL has activity as the best antioxidant, with an IC_{50} value of 57.16 mg/L. These results indicate that the ethanol extract has the strongest antioxidant activity and is ready to be developed as an alternative natural antioxidant [20].

The medication that causes liver damage is a combination of isoniazid and rifampin. The poisonous metabolite of isoniazid, mono acetyl hydrazid (MAH), is responsible for the majority of liver damage. Isoniazid is primarily removed via the liver by acetylation by N-acetyl transferase-2 (NAT-2). Acetyl isoniazid is predominantly converted to mono-acetyl hydrazine and diacetyl hydrazine and other minor metabolites [21]. Acetylation of acetyl isoniazid causes the formation of monoacetyl hydrazine, a potent hepatotoxic toxin in experimental animals. Microsomal metabolism of monoacetyl hydrazine generates reactive acylating chemicals that can bind covalently to tissue macromolecules and cause hepatic necrosis [22].

Microscopic investigations revealed abnormalities in liver histology in the negative group (Figure 2A), including hydrophilic degeneration, fat degeneration, sinusoid congestion, and vascular congestion. The positive group (Figure 2B) showed fatty deterioration, sinusoidal dilatation, and little inflammation. Thus, compared to the negative group, the positive group experienced reduced liver cell damage. The positive group took Curliv®, a herbal supplement that can heal liver damage produced by the induction of isoniazid and rifampin drugs. This implies that the research undertaken was reliable.

The extract group showed hydrophilic degradation, sinusoidal dilatation, and mild inflammation at 100 mg/kg BW (Figure 2C). The results were identical to those seen in the positive group. The EEJL group dose of 200 mg/kg BW resulted in sinusoidal dilatation with inflammation (Figure 2D), whereas the EEJL group dose of 300 mg/kg BW resulted in just sinusoidal dilatation. As a result, the EEJL group dose of 300 mg/kg BW outperformed the group doses of 100 and 200 mg/kg BW in terms of liver damage repair or minimization.

The process of hepatocyte destruction initiates with degeneration. The degeneration that developed was primarily hydrophilic, as seen in the negative group. Hydrophilic degeneration is reversible damage in response to non-lethal injury, characterized by cytoplasmic swelling [23,24]. This is caused by a disturbance in active transport, which prevents cells from pumping Na^+ ions out, resulting in a rise in the concentration of Na^+ ions in cells. Cytoplasmic swelling is a sign of excessive fluid accumulation caused by cells' failure to maintain homeostasis [25]. Furthermore, changes in the cell membrane's and cytoplasmic membrane's characteristics disrupt the cell's integrity, resulting in cell damage. Injured cells generate numerous mediators to initiate the inflammatory process and recruit inflammatory cells [23].

The inflammatory process, also known as the inflammatory reaction, is an important mechanism the body uses to defend itself against various dangers that disrupt equilibrium while also improving the structure and function of the tissue affected by these hazards [26]. The inflammatory process was found in the histology of mice in the positive control group, with EEJL dosages of 100 mg/kg BW and 200 mg/kg BW.

Observations revealed that sinusoidal dilatation occurred in all groups. Sinusoids are small blood veins that function as capillaries in the liver. Sinusoidal dilatation of the liver refers to the expansion of hepatic capillaries. This syndrome is caused by a restriction of the hepatic venous outflow, which results in vascular stasis and hepatic parenchymal congestion. This sinusoidal dilatation is frequently seen when the liver is inflamed owing to illness or drug

usage. Other histological alterations include congestion. Congestion is an accumulation of blood in the hepatic veins caused by blood flow [27].

Based on the results, the EEJL has an effect in repairing and minimizing liver cell damage in rats, which is induced by isoniazid-rifampin, and EEJL, a dose of 300 mg/kg BW, which has the best effect on treating liver cell damage.

3.2. Molecular docking.

Resolution-based selection of 1HD2 and 3NT1 receptors. A resolution value of less than 3Å suggests increased stability during molecular docking [28]. The enzyme is first separated from the native ligand and water so that it does not interfere with the test ligand's binding to the receptor [29]. This is followed by optimization by adding polar hydrogen atoms to approach the body's pH [30] and adding Gasteiger charges to adjust the docking atmosphere so that it can produce correct calculations [31].

Validation of docking between test receptor and native ligand to obtain RMSD (Root Mean Square Deviation) and binding site values. RMSD shows deviations in ligand structure before and after docking [28]. The results obtained for the 1HD2 and 3NT1 receptors were 0.28 and 0.37, respectively. The best RMSD result is ≤2; thus, the results meet the requirements, and the method used is declared valid.

After the docking approach has been confirmed valid, the molecular docking simulation can proceed. The receptors employed are 1HD2 and 3NT1, which use the same binding site as the natural ligand (Figure 3). A binding site is a cavity on the surface of a protein that acts as a place for a ligand to attach. The 1HD2 receptor binding site is center x = 7.088; center y= 41.659; center z= 34.385. Meanwhile, the binding site for the 3NT1 receptor is center x = -31.644; center y= -29.694; center z= -67.448. There were 8 test ligands and native ligands as a comparison. Docking is carried out using AutoDock Vina software following the previous study with slight modifications [32].

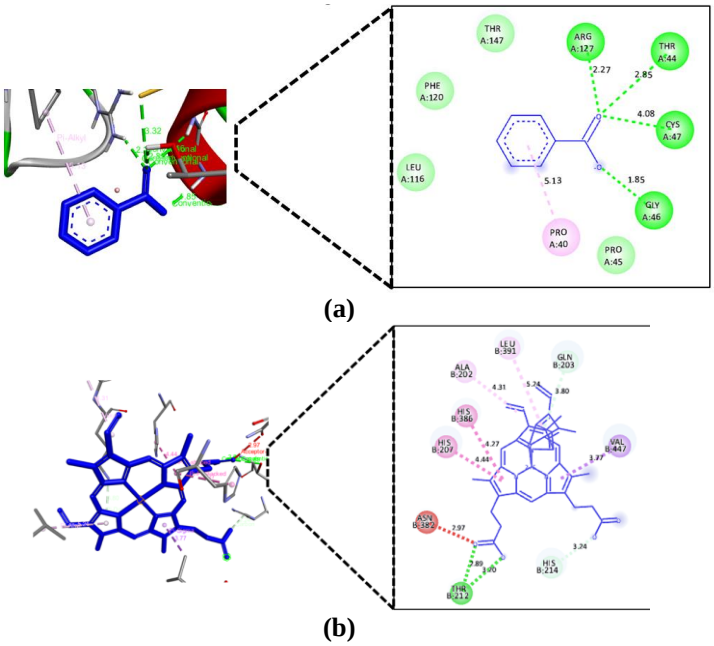

Figure 3. Molecular docking interaction of native ligand toward receptor **(a)** 1HD2; **(b)** 3NT1.

The docking results between the receptor and the test ligand produce Gibbs free energy (ΔG). The result ΔG is a conformational stability parameter between the receptor and the

ligand. Metabolic reactions in the body in terms of thermodynamics take place exergonic and endergonic. Exergonic reactions produce ΔG, which is used to work at a constant temperature and pressure. Exergonic reactions cause the free energy of reactant molecules to decrease because free energy is released during the reaction. Therefore, the ΔG of the product is lower than the ΔG of the reactant. The lower the ΔG of a molecule, the more stable the molecule is, and the reaction proceeds spontaneously.

The ΔG produced between the test ligands toward 1HD2 is at a lower level (-6.134 to -6.881 kcal/mol) compared to the native ligand, which is only -4.701 kcal/mol. These results show the stability of

the interaction between the test ligand and the 1HD2 receptor compared to the native ligand, as shown in Table 1. The molecular interaction of ligand 4 toward 1HD2 and ligand 7 toward 3NT1 is the most stable ligand among all test ligands shown in Figure 4. The other ligands are shown in Figures S1 and S2 in the Supporting Information. Besides, the interaction of the native ligand toward the 3NT1 receptor showed more stability than test ligands.

Table 1. Gibbs free energy (ΔG) of ligands toward the receptor

Model	ΔG - 1HD2 (kcal/mol)	ΔG - 3NT1 (kcal/mol)
Native ligand	-4.701	-17.82
1	-6.499	-8.854
2	-6.314	-8.517
3	-6.328	-8.366
4	-6.881	-8.532
5	-6.726	-8.823
6	-6.737	-8.729
7	-6.702	-9.061
8	-6.615	-8.555

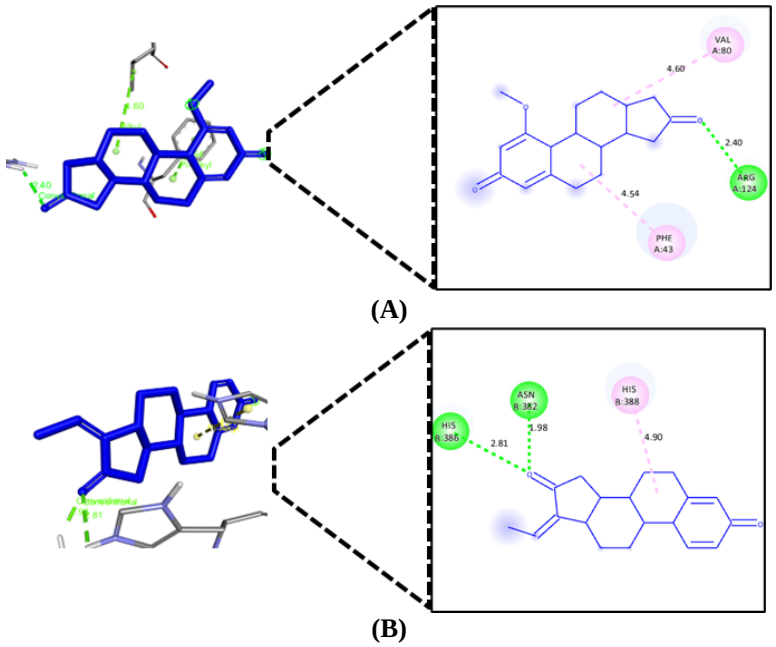

Figure 4. Molecular docking interaction of ligand 4 toward receptor **(a)** 1HD2; **(b)** ligand 7 toward 3NT1.

Apart from Gibbs free energy, the presence of similar interaction types, such as the formation of hydrogen bonds or involvement of specific amino acid residues in ligand-receptor interactions, suggests comparable activities [33,34]. Table 2 shows that one of the van der Walls interactions with the native ligand, PHE120, is involved in the interaction. This is found in several other test ligands, such as 6, 7, and 8. The strength of an interaction between a ligand

and a protein amino acid is determined by the distance between them. An interaction is considered strong if the distance is between 3.0 Å and 5.0 Å, and weak if it exceeds 5.0 Å [35,36].

Table 2. Interaction of ligands in complex with the receptor 1HD2.

Model	Hydrogen bonds			Hydrophobic interactions		
	Residue	AA	Distance (Å)	Residue	AA	Distance (Å)
Native ligand	127	ARG	2.27	40	PRO	5.13
	47	CYS	4.08	-	-	-
	46	GLY	1.85	-	-	-
	44	THR	2.85	-	-	-
1	-	-	-	43	PHE	4.47
2	-	-	-	43	PHE	4.48
3	124	ARG	2.40	43	PHE	4.54
	-	-	-	80	VAL	4.60
4	124	ARG	6.00	43	PHE	4.40; 3.74
	76	ASN	2.25; 5.17	-	-	-
5	124	ARG	6.04	43	PHE	3.76; 4.82
	76	ASN	2.27; 5.18	80	VAL	4.59
6	-	-	-	43	PHE	3.75; 5.36
	-	-	-	120	PHE	5.12
	-	-	-	80	VAL	4.86
7	124	ARG	4.94	43	PHE	3.70
	76	ASN	2.32	120	PHE	6.51
	-	-	-	80	VAL	4.7
8	76	ASN	5.35	120	PHE	5.01
	-	-	-	80	VAL	3.62

The docking results between the test ligand and the 3NT1 receptor (Table 3) showed differences compared to the native ligand, where the best test ligand was test ligand 7, with an energy value of -9.061 kcal/mol. Meanwhile, the native ligand has a lower energy value, namely -17.82. These results show that the test ligand has potential as an anti-inflammatory because the interaction with COX-1 gave negative results, which means the reaction occurred spontaneously. However, it is not better or more stable than the native ligand.

Table 3. Interaction of ligands in complex with the receptor 3NT1.

Model	Hydrogen bonds			Hydrophobic interactions		
	Residue	AA	Distance (Å)	Residue	AA	Distance (Å)
Native ligand	203	GLN	3.80	202	ALA	4.31
	214	HIS	3.24	207	HIS	4.44
	212	THR	3.20	386	HIS	4.27
	-	-	-	391	LEU	5.24
	-	-	-	447	VAL	3.77
1	-	-	-	391	LEU	5.07
	-	-	-	388	HIS	5.48; 4.28
	-	-	-	207	HIS	5.35
2	-	-	-	391	LEU	5.10
	-	-	-	388	HIS	5.41; 3.88
	-	-	-	207	HIS	5.34
3	382	HIS	1.92	207	HIS	4.44; 5.38
	386	HIS	2.69	388	HIS	4.44; 4.86
4	382	HIS	2.05	207	HIS	4.49
	386	HIS	2.96	-	-	-
	388	HIS	2.17	-	-	-
5	382	ASN	2.09	202	ALA	3.34
	386	HIS	2.89	207	HIS	4.41
	388	HIS	2.23	390	LEU	4.99
	-	-	-	387	TRP	4.30
6	388	HIS	4.90	382	ASN	1.98
	-	-	-	386	HIS	2.81
7	-	-	-	388	HIS	5.18
	-	-	-	294	LEU	5.04

Model	Hydrogen bonds			Hydrophobic interactions		
	Residue	AA	Distance (Å)	Residue	AA	Distance (Å)
	-	-	-	391	LEU	5.16
	-	-	-	408	LEU	4.84
	-	-	-	444	VAL	5.32
8	-	-	-	385	TYR	3.32

The interaction results show that the similarity of the binding amino acids such as ALA202, HIS207, HIS386, and LEU391 to the native ligand is found in several test ligands. The similarity of amino acid interactions indicates the similarity of activity.

All test ligands have potential as antioxidants because the interaction between the test ligand and the 1HD2 receptor has a lower Gibbs free energy compared to the native ligand. However, in terms of amino acid interactions, there is only one similarity, namely PHE120, which is also found in several of the tested ligands. The Gibbs free energy produced between the ligand and the 3NT1 receptor is suboptimal compared to the native ligand. However, there are many similarities in amino acid interactions, such as ALA202, HIS207, HIS386, and LEU391 in the native ligand found in several of the tested ligands.

4. Conclusion

The findings of the histopathology test revealed that the EEJL affected the repairing of the structure of injured liver cells in rats. Histological examination demonstrated that the EEJL group dose of 300 mg/kg BW had a greater effect than the other groups since only sinusoidal dilation was observed in the liver segment. The hepatoprotective efficacy of EEJL is due to its active compound in *Arthocarpus heterophyllus* Lam. ability to serve as an anti-inflammatory and antioxidant via hydrophilic and hydrophobic interactions with 1HD2 and 3NT1 corresponding to antioxidant and COX-1 receptors, respectively.

Funding

This work was supported by the Faculty of Pharmacy, Universitas Muslim Indonesia.

Acknowledgments

The authors acknowledge the Molecular Probes Discovery Unit, Faculty of Pharmacy, Universitas Muslim Indonesia, for their support and encouragement in carrying out this research.

Conflicts of Interest

The authors declare no conflict of interest.

References

1. Chakaya, J.; Khan, M.; Ntoumi, F.; Aklillu, E.; Fatima, R.; Mwaba, P.; Kapata, N.; Mfinanga, S.; Hasnain, S.E.; Katoto, P.D.M.C.; Bulabula, A.N.H.; Sam-Agudu, N.A.; Nachega, J.B.; Tiberi, S.; McHugh, T.D.; Abubakar, I.; Zumla, A. Global Tuberculosis Report 2020 – Reflections on the Global TB burden, treatment and prevention efforts. *Int. J. Infect. Dis.* **2021**, *113*, S7-S12, https://doi.org/10.1016/j.ijid.2021.02.107.
2. Wang, Y.-C.; Chen, K.-H.; Chen, Y.-L.; Lin, S.-W.; Liu, W.-D.; Wang, J.-T.; Hung, C.-C. Pyrazinamide related prolonged drug-induced liver injury: A case report. *Medicine* **2022**, *101*, e30955, https://doi.org/10.1097/md.0000000000030955.

3. Shen, T.; Liu, Y.; Shang, J.; Xie, Q.; Li, J.; Yan, M.; Xu, J.; Niu, J.; Liu, J.; Watkins, P.B.; Aithal, G.P.; Andrade, R.J.; Dou, X.; Yao, L.; Lv, F.; Wang, Q.; Li, Y.; Zhou, X.; Zhang, Y.; Zong, P.; Wan, B.; Zou, Z.; Yang, D.; Nie, Y.; Li, D.; Wang, Y.; Han, X.a.; Zhuang, H.; Mao, Y.; Chen, C. Incidence and Etiology of Drug-Induced Liver Injury in Mainland China. *Gastroenterology* **2019**, *156*, 2230-2241.e2211, https://doi.org/10.1053/j.gastro.2019.02.002.
4. Devarbhavi, H.; Singh, R.; Patil, M.; Sheth, K.; Adarsh, C.K.; Balaraju, G. Outcome and determinants of mortality in 269 patients with combination antituberculosis drug-induced liver injury. *J. Gastroenterol. Hepatol.* **2013**, *28*, 161-167, https://doi.org/10.1111/j.1440-1746.2012.07279.x.
5. Hammad, M.; Raftari, M.; Cesário, R.; Salma, R.; Godoy, P.; Emami, S.N.; Haghdoost, S. Roles of Oxidative Stress and Nrf2 Signaling in Pathogenic and Non-Pathogenic Cells: A Possible General Mechanism of Resistance to Therapy. *Antioxidants* **2023**, *12*, 1371, https://doi.org/10.3390/antiox12071371.
6. Hou, W.; Nsengimana, B.; Yan, C.; Nashan, B.; Han, S. Involvement of endoplasmic reticulum stress in rifampicin-induced liver injury. *Front. Pharmacol.* **2022**, *13*, 1022809, https://doi.org/10.3389/fphar.2022.1022809.
7. Zhuang, X.; Li, L.; Liu, T.; Zhang, R.; Yang, P.; Wang, X.; Dai, L. Mechanisms of isoniazid and rifampicin-induced liver injury and the effects of natural medicinal ingredients: A review. *Front. Pharmacol.***2022**, *13*, 1037814, https://doi.org/10.3389/fphar.2022.1037814.
8. Hong, M.; Li, S.; Tan, H.Y.; Wang, N.; Tsao, S.-W.; Feng, Y. Current Status of Herbal Medicines in Chronic Liver Disease Therapy: The Biological Effects, Molecular Targets and Future Prospects. *Int. J. Mol. Sci.* **2015**, *16*, 28705-28745, https://doi.org/10.3390/ijms161226126.
9. Sreeja Devi, P.S.; Kumar, N.S.; Sabu, K.K. Phytochemical profiling and antioxidant activities of different parts of *Artocarpus heterophyllus* Lam. (Moraceae): A review on current status of knowledge. *Future J. Pharm. Sci.* **2021**, *7*, 30, https://doi.org/10.1186/s43094-021-00178-7.
10. Yusuf, M.I.; Susanty, S.; Fawwaz, M. Antioxidant and antidiabetic potential of galing stem extract (*Cayratia trifolia* Domin). *Pharmacogn. J.* **2018**, *10*, 686-689, https://doi.org/10.5530/pj.2018.4.113.
11. Fawwaz, M.; Purwono, B.; Sidiq, Y.; Arwansyah; Arsul, M.I.; Fitriana; Pratama, M.; Fajriani, A.; Kusuma, A.T.; Amirullah; et al. Anti-inflammatory, Antioxidant, and Antibacterial Activities with Molecular Docking Studies of *Vitex trifolia* L. Targeting Human COX-2 and Peroxiredoxin-5. *ChemistrySelect* **2024**, *9*, e202403834, https://doi.org/10.1002/slct.202403834.
12. Mawardika, H.; Wahyuni, D.; Khasanah, S.M. Antibacterial Potency of Jackfruit Leaf Extract (*Artocarpus heterophyllus* L.) Against *Salmonella typhi*. *Pharmacon: Jurnal Farmasi Indonesia* **2023**, 20, 195-204, https://doi.org/10.23917/pharmacon.v20i2.20862.
13. Widyawati, T.; Daulay, M. Effect of Using Ethanol Extract of Artocarpus Heterophyllus Leaves and Olea Europea Fruit Oil Combination on Facial Skin. *Acta Inform. Med.* **2023**, *31*, 168-171, https://doi.org/10.5455/aim.2023.31.168-171.
14. Kiernan, J. Histological and histochemical methods, 5th Edition; Scion publishing ltd: **2015**.
15. Tien; Utami, T.W.; Aritrina, P.; Kardin, L.; Sukurni; Syarifin, A.N.K.; Subangkit, M. Histopathological analysis of the liver in hypercholesterolemia rats treated with *Dillenia serrata* fruits. *Acta Biochim. Indon.* **2023**, *5*, 85.
16. Trott, O.; Olson, A.J. AutoDock Vina: Improving the speed and accuracy of docking with a new scoring function, efficient optimization, and multithreading. *J. Comput. Chem.* **2010**, *31*, 455-461, https://doi.org/10.1002/jcc.21334.
17. Liu, Y.-Y.; Wang, T.; Yang, R.-X.; Tang, H.-X.; Qiang, L.; Liu, Y.-P. Anti-inflammatory steroids from the fruits of *Artocarpus heterophyllus*. *Nat. Prod. Res.* **2021**, *35*, 3071-3077, https://doi.org/10.1080/14786419.2019.1693562.
18. Fawwaz, M.; Mishiro, K.; Purwono, B.; Nishii, R.; Ogawa, K. Synthesis and evaluation of a rociletinib analog as prospective imaging double mutation L858R/T790M in non-small cell lung cancer. *J. Pharm. Pharmacogn. Res.* **2024**, *12*, 231-242, https://doi.org/10.56499/jppres23.1743_12.2.231.
19. Mbaeyi-Nwaoha, I.E.; Onwuka, C.P. Comparative evaluation of antimicrobial properties and phytochemical composition of Artocarpus altilis leaves using ethanol, n-hexane and water. *Afr. J. Microbiol. Res.* **2014**, *8*, 3409-3421, http://dx.doi.org/10.5897/AJMR2014.6930.
20. Yunita, D.S. Testing The Antioxidant Activity of The Ethanol Extract of Jackfruit Leaves (Artocarpus heterophyllus) Using The DPPH Method. Universitas Sumatera Utara, Medan - Indonesia, **2023**.

21. Saukkonen, J.J.; Cohn, D.L.; Jasmer, R.M.; Schenker, S.; Jereb, J.A.; Nolan, C.M.; Peloquin, C.A.; Gordin, F.M.; Nunes, D.; Strader, D.B. An Official ATS Statement: Hepatotoxicity of Antituberculosis Therapy. *Am. J. Respir. Crit. Care Med.* **2006**, *174*, 935-952, https://doi.org/10.1164/rccm.200510-1666ST.
22. AHFS. AHFS Drug Information; American Society of Health-System Pharmacist: Bethesda, **2005**.
23. Andreas, H.; Trianto, H.F.; Ilmiawan, M.I. *Gambaran Histologi Regenerasi Hati Pasca Penghentian Pajanan Monosodium Glutamat pada Tikus Wistar*. *eJournal Kedokteran Indonesia* **2015**, *3*, https://dx.doi.org/10.23886/ejki.3.4804.
24. Miller, M.A.; Zachary, J.F. Mechanisms and Morphology of Cellular Injury, Adaptation, and Death. *Pathologic Basis of Veterinary Disease.* **2017**, *17*, https://doi.org/10.1016/B978-0-323-35775-3.00001-1.
25. Myers, R.; McGavin, M.D. Cellular and Tissue Responses to Injury. In Pathologic Basis of Veterinay Disease, Fourth Edition; McGavin, M.D., Zachary, J.F, Eds.; Elsevier Health Sciences, **2007**.
26. Suparman, I.P.; Sudira, I.W.; Berata, I.K. Kajian Ekstrak Daun Kedondong (*Spondias dulcis* G.Forst.) Diberikan Secara Oral Pada Tikus Putih Ditinjau Dari Histopatologi Ginjal. *Buletin Veteriner Udayana* **2013**, *5*.
27. Brancatelli, G.; Furlan, A.; Calandra, A.; Dioguardi Burgio, M. Hepatic sinusoidal dilatation. *Abdom. Radiol.* **2018**, *43*, 2011-2022, https://doi.org/10.1007/s00261-018-1465-8.
28. Dwitiyanti, D.; Rachmania, R.A.; Efendi, K.; Septiani, R.; Jihadudin, P. *In Vivo* Activities and *In Silico* Study of Jackfruit Seeds (*Artocarpus heterophyllus* Lam.) on the Reduction of Blood Sugar Levels of Gestational Diabetes Rate Induced by Streptozotocin. *Open Access Maced. J. Med. Sci.* **2019**, *7*, 3819-3826.
29. Rena, S.R.; Nurhidayah, N.; Rustan, R. Analisis Molecular Docking Senyawa Garcinia Mangostana L Sebagai Kandidat Anti SARS-CoV-2. *Jurnal Fisika Unand* **2022**, *11*, 82-88.
30. Sari, I.W.; Junaidin, J.; Pratiwi, D. Studi Molecular Docking Senyawa Flavonoid Herba Kumis Kucing (*Orthosiphon stamineus* B.) Pada Reseptor a-Glukosidase Sebagai Antidiabetes Tipe 2. *Jurnal Farmagazine* **2020**, *7*, 54.
31. Noviardi, H.; Masaenah, E.; Ramadhan, R. Penapisan Molekular Kandidat Obat Sintetik Tuberkulosis Terhadap Protein Tirosin Kinase Mycobacterium tuberculosis. *Pharmamedika Journal* **2020**, *5*, 60-69, https://doi.org/10.47219/ath.v5i2.104.
32. Fawwaz, M.; Mishiro, K.; Arwansyah, A.; Nishii, R.; Ogawa, K. Synthesis and initial *in vitro* evaluation of olmutinib derivatives as prospective imaging probe for non-small cell lung cancer. *Bioimpacts* **2024**, *14*, 27774, https://doi.org/10.34172/bi.2023.27774.
33. Mohanty, M.; Mohanty, P.S. Molecular docking in organic, inorganic, and hybrid systems: a tutorial review. *Monatsh. Chem. – Chem. Monthly* **2023**, *154*, 683-707, https://doi.org/10.1007/s00706-023-03076-1.
34. Alam, M. Exploration of Binding Affinities of a 3β,6β-Diacetoxy-5α-cholestan-5-ol with Human Serum Albumin: Insights from Synthesis, Characterization, Crystal Structure, Antioxidant and Molecular Docking. *Molecules* **2023**, *28*, 5942, https://doi.org/10.3390/molecules28165942.
35. Zhan, J.; Lei, Z.; Zhang, Y. Non-covalent interactions of graphene surface: Mechanisms and applications. *Chem* **2022**, *8*, 947-979, https://doi.org/10.1016/j.chempr.2021.12.015.
36. Tam, J.Z.; Palumbo, T.; Miwa, J.M.; Chen, B.Y. Analysis of Protein-Protein Interactions for Intermolecular Bond Prediction. *Molecules* **2022**, *27*, 6178, https://doi.org/10.3390/molecules27196178.

Supplementary materials

Native ligand

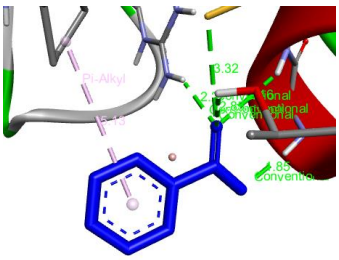

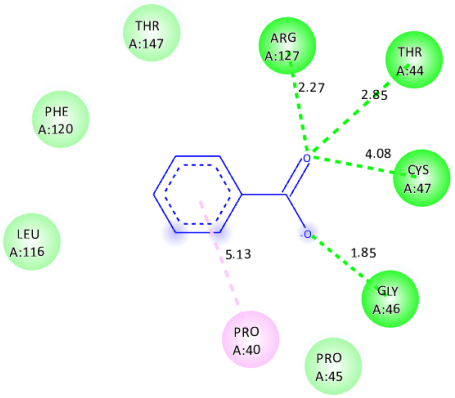

Ligand 1

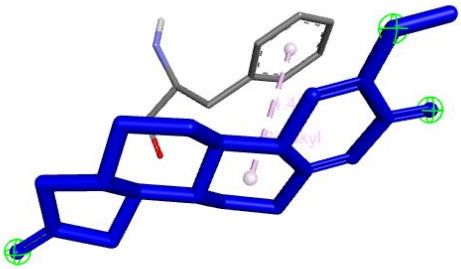

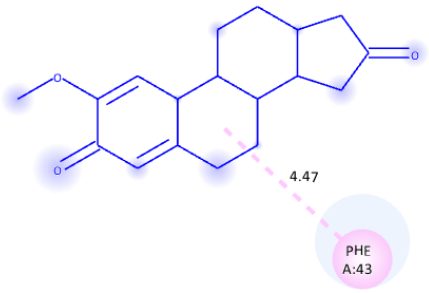

Ligand 2

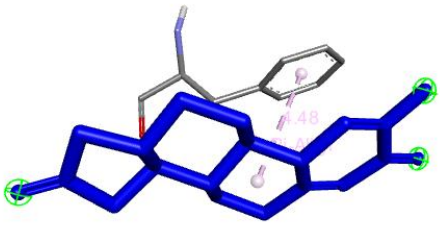

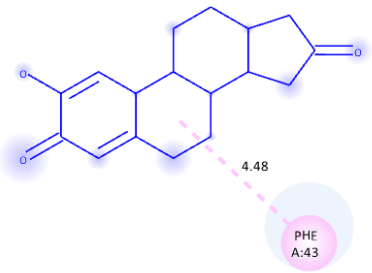

Ligand 3

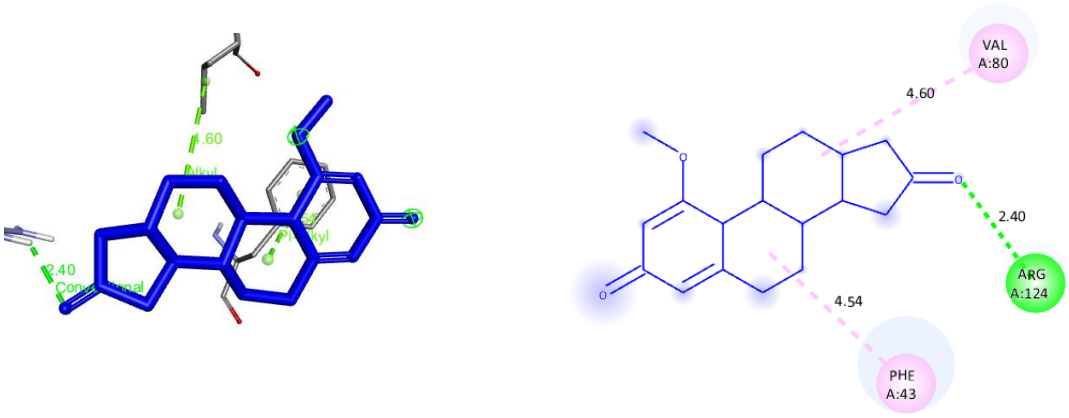

Ligand 4

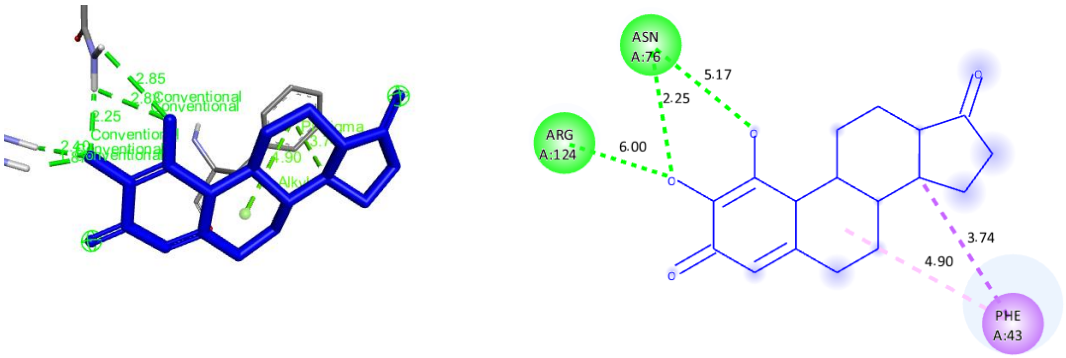

Ligand 5

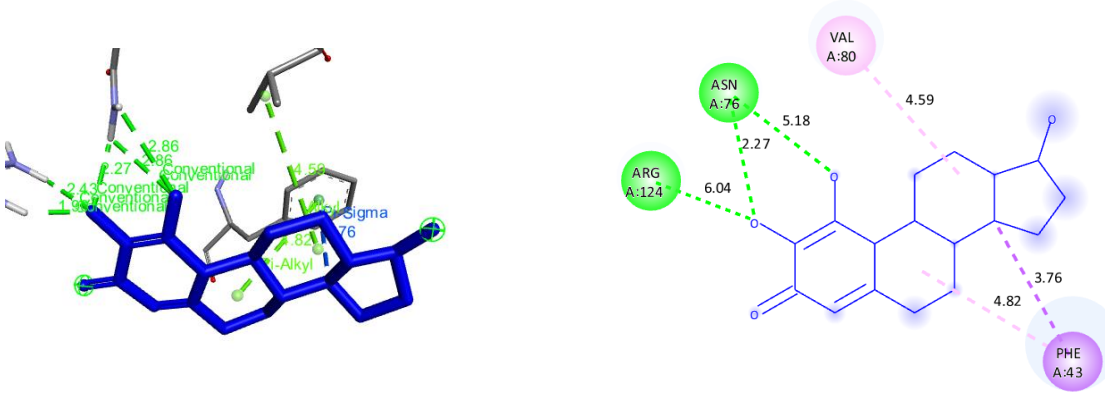

Ligand 6

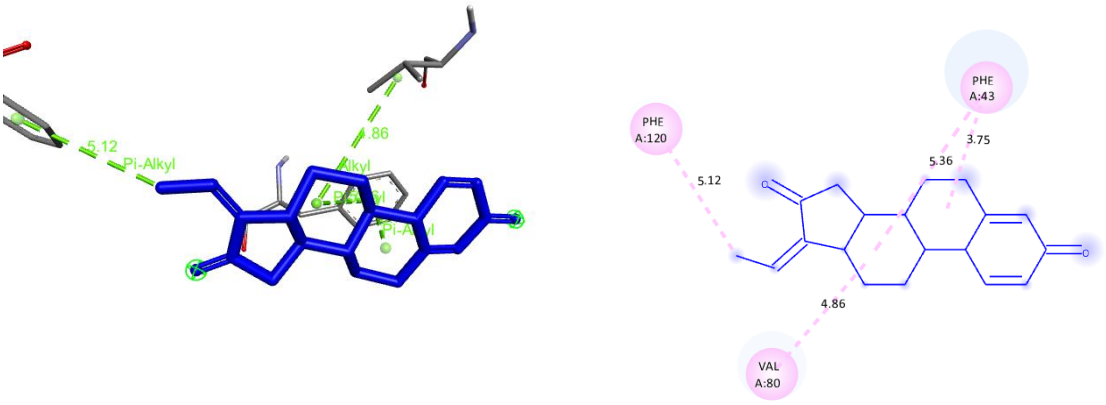

Ligand 7

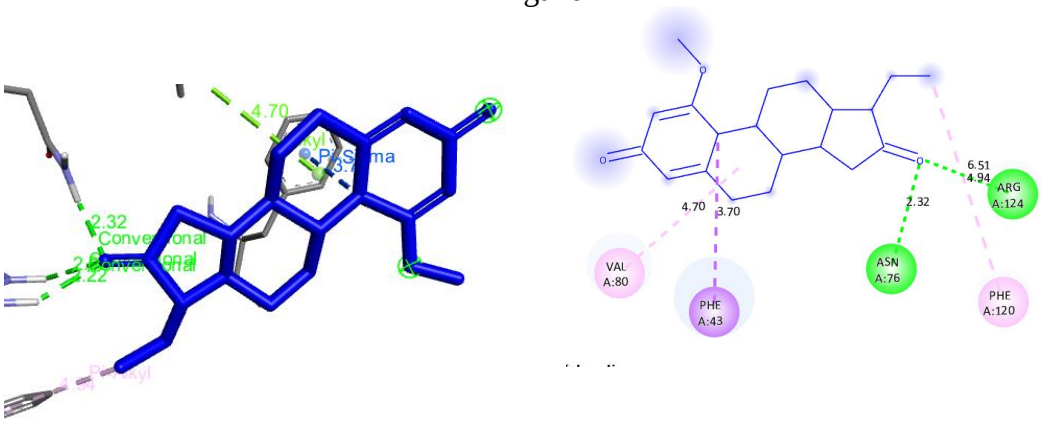

Ligand 8

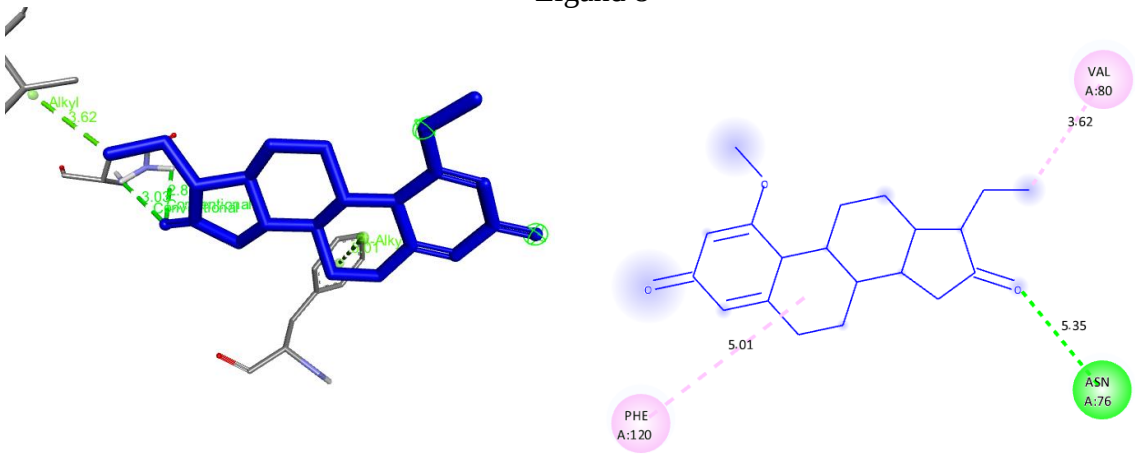

Figure S1. Molecular docking of ligands toward 1HD2.

Native Ligand

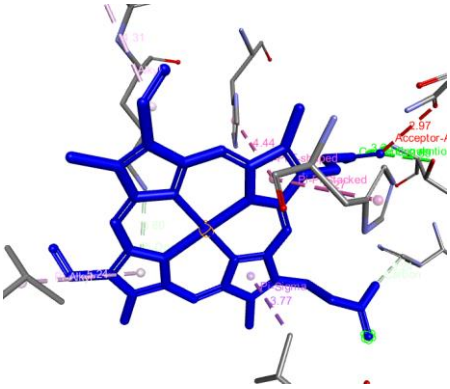

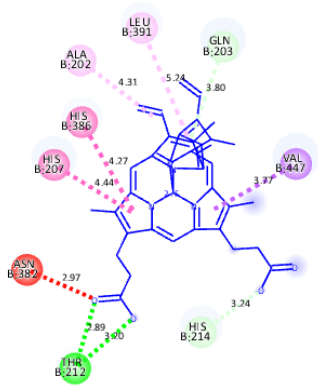

Ligand 1

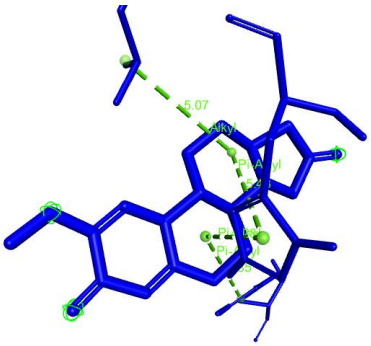

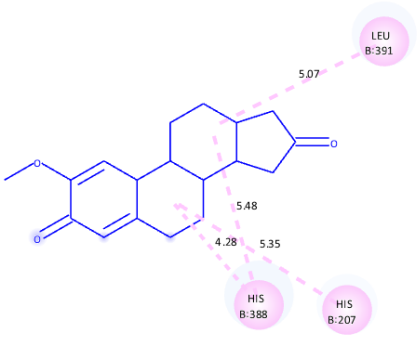

Ligand 2

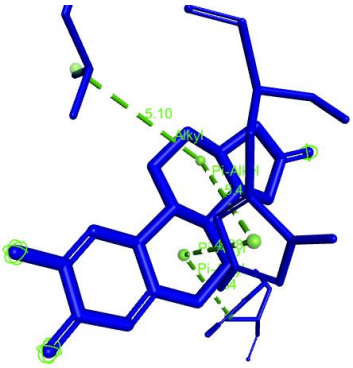

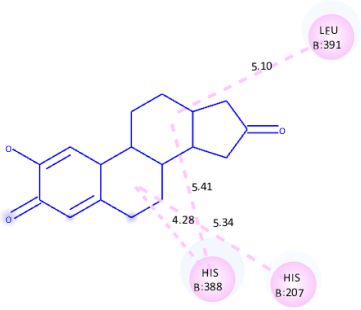

Ligand 3

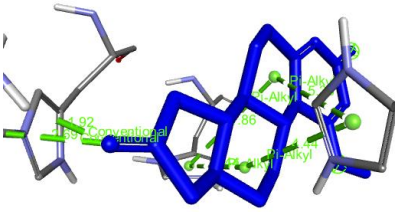

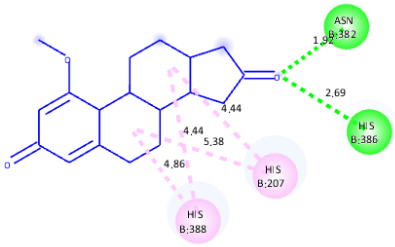

Ligand 4

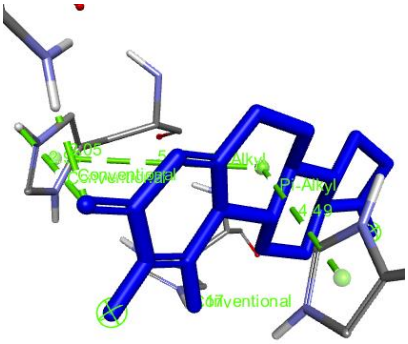

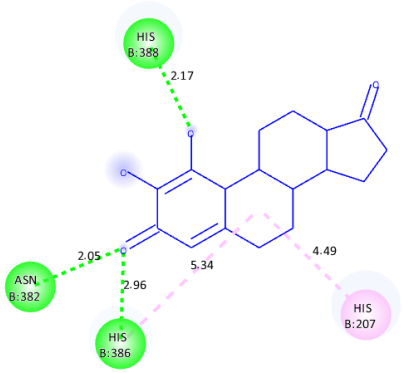

Ligand 5

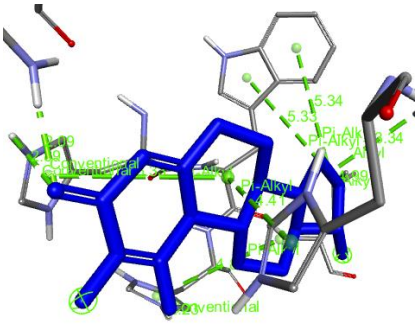

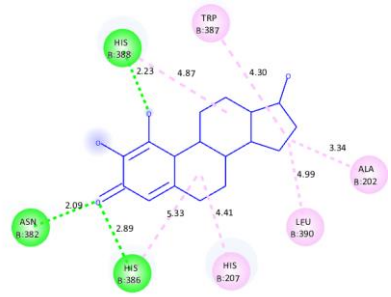

Ligand 6

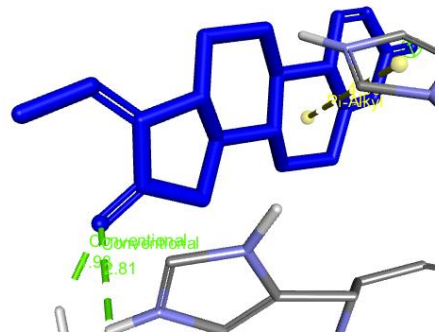

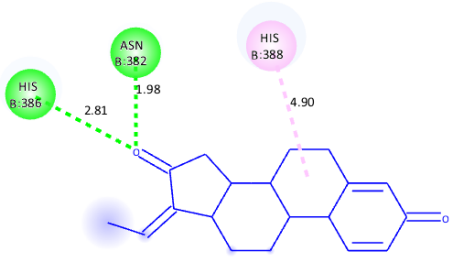

Ligand 7

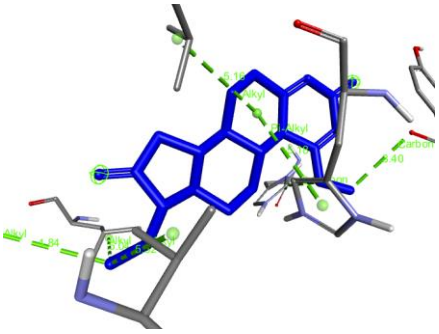

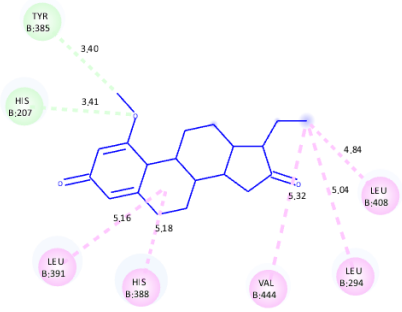

Ligand 8

Figure S2. Molecular docking of ligandds toward 3NTI1.